Stability, Folding, Dimerization, and Assembly Properties of the Yeast Prion Ure2p†

Carine Thual,[||,#] Luc Bousset,[||,#] Anton A. Komar,[⊥,§] Stefan Walter,[‡] Johannes Buchner,[‡] Christophe Cullin,[⊥] and Ronald Melki*[,#]

Laboratoire d'Enzymologie et Biochimie Structurales and Centre de Génétique Moléculaire, Centre National de la Recherche Scientifique, 91198 Gif-sur-Yvette Cedex, France, and Institut fuer Organische Chemie und Biochemie, Technische Universitaet Muenchen, D-85747 Garching, Germany

Received August 14, 2000; Revised Manuscript Received November 27, 2000

ABSTRACT: The [URE3] factor of *Saccharomyces cerevisiae* propagates by a prion-like mechanism and corresponds to the loss of the function of the cellular protein Ure2. The molecular basis of the propagation of this phenotype is unknown. We recently expressed Ure2p in *Escherichia coli* and demonstrated that the N-terminal region of the protein is flexible and unstructured, while its C-terminal region is compactly folded. Ure2p oligomerizes in solution to form mainly dimers that assemble into fibrils [Thual et al. (1999) *J. Biol. Chem. 274*, 13666−13674]. To determine the role played by each domain of Ure2p in the overall properties of the protein, specifically, its stability, conformation, and capacity to assemble into fibrils, we have further analyzed the properties of Ure2p N- and C-terminal regions. We show here that Ure2p dimerizes through its C-terminal region. We also show that the N-terminal region is essential for directing the assembly of the protein into a particular pathway that yields amyloid fibrils. A full-length Ure2p variant that possesses an additional tryptophan residue in its N-terminal moiety was generated to follow conformational changes affecting this domain. Comparison of the overall conformation, folding, and unfolding properties, and the behavior upon proteolytic treatments of full-length Ure2p, Ure2pW37 variant, and Ure2p C-terminal fragment reveals that Ure2p N-terminal domain confers no additional stability to the protein. This study reveals the existence of a stable unfolding intermediate of Ure2p under conditions where the protein assembles into amyloid fibrils. Our results contradict the intramolecular interaction between the N- and C-terminal moieties of Ure2p and the single unfolding transitions reported in a number of previous studies.

There are at least two natural genetic elements in budding yeast *Saccharomyces cerevisiae* that exhibit non-Mendelian inheritance but can be "cured" by treatment of the cells with low concentrations of the protein denaturant guanidine hydrochloride and reappear without introduction of new DNA (*1*). [URE3] is one of these elements. It was discovered 25 years ago (*2*−*3*). This element is inherited in a dominant, cytoplasmic fashion. Several lines of evidence suggest that [URE3] is due to a protein, Ure2p (reviewed in refs *1* and *4*). Because of the conceptual similarities between the mode of transmission of [URE3] and that of the infectious agent in mammalian prion diseases, it has been proposed that [URE3] is a yeast prion (*5*).

The prion concept originates from studies of transmissible spongiform encephalopathies, where numerous lines of evidence indicate that the infectious agents causing these diseases are proteins rather than viruses or nucleic acids (*6*). A protein-only model was proposed to account for the propagation of this class of diseases in which a constitutive membrane protein (PrP^{c}) is subject to a conformational alteration (PrP^{sc}) that enables it to convert, in a catalytic fashion, the constitutive form of the protein into its scrapie-associated form.

Despite active research on the structure, the biochemical properties, the role of cellular ligands, and the mechanism of propagation of the mammalian prions, a number of questions remain unanswered. The prion-like phenomenon [URE3] of the yeast *S. cerevisiae* provides a powerful model system to address a number of these questions. For example, what is the contribution of Ure2p structural domains on a number of biochemical properties of the molecule, such as the stability, the conformation, the capacity to assemble into amyloid fibrils, and the function.

On the basis of genetic and biochemical studies, Ure2p has been shown to be a two-domain protein (*7*−*9*). The poorly structured (*9*) N-terminal portion of the protein is required for the expression of prion phenotype (*7*) and is involved in the aggregation of the protein (*10*−*12*). The compactly folded (*9*, *13*) C-terminal moiety of Ure2p fully

† This work was supported by grants from the Centre National de la Recherche Scientifique, the Association pour la Recherche sur le Cancer and the Actions Concertées Program of the French Ministry of Research and Technology. A.A.K. and C.T. were supported by the Fondation pour la Recherche Médicale.

* Corresponding author. Phone: 33 1 69 82 35 03. Fax: 33 1 69 82 31 29. E-mail: Ronald.Melki@lebs.cnrs-gif.fr.

[#] Laboratoire d'Enzymologie et Biochimie Structurales, Centre National de la Recherche Scientifique.

[||] The first two authors contributed equally to this work.

[⊥] Centre de Génétique Moléculaire, Centre National de la Recherche Scientifique.

[‡] Technische Universitaet Muenchen.

[§] Present address: Institut fuer Biochemie und Molekularbiologie Universitaet Bern, Buehlstr. 28, 3012 Bern, Switzerland.

10.1021/bi001916l CCC: $20.00
Published on Web 01/19/2001

complements *URE2* gene deletion and shares a low degree of sequence homology with the glutathione *S*-transferase (GST) family (*14*). It has been proposed that Ure2p N- and C-terminal regions interact specifically with each other. The interaction is greatly enhanced when the two domains are covalently bound (*7*, *8*, *15*), suggesting that the interaction is intramolecular.

To determine the exact role of each domain of Ure2p on the overall properties of the protein, specifically, its stability, conformation, and capacity to assemble into amyloid fibrils, Ure2p N- and C-terminal domains were expressed separately. We have attempted their purification. While Ure2p N-terminal fragment (extending from amino acid residues 1−93) degrades when expressed alone or fused to an intein-chitin binding domain chimera [IMPACT T7 system, New England Biolabs, Inc.], the C-terminal region of the protein was successfully purified. Ure2p 95−354 is dimeric, as is full-length Ure2p, which indicates that the dimerization process does not involve the Ure2p N-terminal moiety. Ure2p 95−354 assembles into insoluble high molecular weight oligomers as does full-length Ure2p. However, unlike authentic Ure2p, the C-terminal region of the protein does not assemble into fibrils and is incapable of being incorporated into such preformed polymers. This underlines the crucial role of the N-terminal fragment of the protein in directing its polymerization into a specific assembly pathway. We demonstrate that the degradation pattern generated upon proteolysis of Ure2p is solely due to the Ure2p 95−354 fragment. To follow conformational changes affecting the N-terminal moiety of the protein, we generated a Ure2p variant (Ure2pW37) in which the phenylalanine residue at position 37 was substituted by a tryptophan. Comparison of the overall conformation, folding, and unfolding properties of wild-type Ure2p, Ure2pW37, and Ure2p 95−354 reveals that Ure2p N-terminal region is unstructured and confers no additional stability to the protein. This finding is in contradiction with the hypothetical intramolecular interaction between the N- and C-terminal moieties of Ure2p (*7*, *8*, *15*). Finally, we bring evidence for an unfolding intermediate under conditions where Ure2p assembles into amyloid fibrils.

EXPERIMENTAL PROCEDURES

Reagents. Ethylene glycol bis-(*β*-aminoethyl ether)-*N*,*N*,*N*′,*N*′-tetraacetic acid (EGTA)[1] and sodium dodecyl sulfate (SDS) were from Sigma. Proteinase K was purchased from Stratagene. Guanidine hydrochloride came from Fluka. Acrylamide and all other electrophoresis reagents were from Bio-Rad. All other chemicals were analytical grade from Merck.

Construction of Ure2p and Ure2pW37 Variant Expression Vectors in E. coli. The full-length Ure2p expression vector (pET-URE2*) was obtained by amplifying by PCR after linearization with *Xmn*I a pBluescript II SK$^+$URE2* construct (*16*) that encodes for Ure2p, in which the rare codons AGA encoding arginine residues at positions 253 and 254 were changed into CGT codons, in the presence of the following primers: 5′-TGATGAATAACAACGGCAACCAAGTG-3′ and 5′-CCGCGGTGGCGGCCGCT-3′. The amplified fragment was digested with *Bam*HI and ligated into a pET3a vector in which the *Nde*I restriction site was first filled in using the Klenow fragment prior to its digestion by *Bam*HI.

The Ure2pW37 variant expression vector was obtained by site-directed mutagenesis by replacing the TTT codon encoding phenylalanine residue at position 37 by a TGG codon encoding a tryptophan. This mutation was achieved as follows: pET-URE2* was linearized with *Xmn*I and the large 3928-bp fragment containing the Ure2 gene was purified and amplified using the upstream 5′-CGGTTTCCCTCTAGAAATAATTTTG-3′ and downstream 5′-CCTGTTGAAAATTCCCAATTTATATTACTTTGATCGG-3′ primers. The PCR product was then purified and used in a second PCR reaction as an upstream primer, the oligonucleotide 5′-TCCGAAAATGCCTGTTGTTGTTGTC-3′ as a downstream primer, and pET-URE2* linearized with *Xmn*I as a template.

The resulting PCR product was digested with *Xba*I and *Not*I and ligated into purified pETUre2p* digested using the same enzymes. This allows the replacement of wild-type *Xba*I−*Not*I URE2 gene by the *Xba*I−*Not*I fragment that encodes the Ure2pW37 variant.

Construction of Ure2p C-Terminal Domain Expression Vector in E. coli. The Ure2p COOH-terminal domain expression vector was prepared as follows: A pBluescript II SK$^+$URE2* construct (*16*) that encodes the Ure2p 94−354 COOH-terminal fragment, in which the rare codons AGA encoding arginine residues at positions 253 and 254 were changed into CGT codons, was linearized with *Xmn*I and amplified using the primers 5′-ATGAGTCACGTGGAGTATTCC-3′ and 5′-CCGCGGTGGCGGCCGCT-3′. The amplified fragment was digested with *Bam*HI and ligated into a pET3a vector in which the *Nde*I restriction site was first filled in using the Klenow fragment prior to its digestion by *Bam*HI.

Expression and Purification of Recombinant Ure2p, Ure2pW37 Variant, and Ure2p C-Terminal Domain. The expression constructs pET-URE2*, pET-URE2*W37, and pET-URE2*94-354 were transformed into the BL21 (DE3) *E. coli* strain. The expression of recombinant proteins and their purification was performed as described (*9*) with the exception that no hydroxyapatite chromatography was required for recombinant Ure2p C-terminal domain. In the latter case, the material emerging from the phenyl-Sepharose (Pharmacia) column was over 97% homogeneous as judged from running a sample on a 10% SDS−polyacrylamide gel. Purified proteins were pooled then frozen in aliquots and stored at −70 °C. The typical yields were 20 mg of wild-type Ure2p and Ure2pW37 variant and 40 mg of Ure2p C-terminal domain per liter of culture.

For analytical ultracentrifugation experiments, electron microscopy, and proteolytic digestions, recombinant proteins were subjected to an additional gel filtration step through a Superose 6 HR 10/30 column (Pharmacia) equilibrated in 50 mM Tris, pH 7.5, 1 mM EGTA.

Sedimentation Velocity and Molecular Mass Determination. Sedimentation velocity experiments were carried out as described (*9*). Measurements were made at 40 000 or 60 000 rpm and 20 °C. Data were analyzed to provide the apparent distributions of sedimentation coefficients by means of the program SVEDBERG (*17*) and DC/DT (*18*).

[1] Abbreviations: SDS, sodium dodecyl sulfate; PAGE, polyacrylamide gel electrophoresis; Tricine, *N*-[2-hydroxy-1,1-bis(hydroxymethyl)ethyl]glycine; CD, circular dichroism.

Equilibrium sedimentation measurements were performed in the same instrument but at 10 °C. Sample volumes of 100 μL were centrifuged at 12 000 rpm. Radial scans of absorbance at 278 nm were taken at 3 h intervals to monitor the attainment of equilibrium. Equilibrium was reached after 24 h of centrifugation. The data were analyzed to yield weight-average molecular weights by the use of the programs XLAEQ and EQASSOC supplied by Beckman. The partial specific volume was calculated from the amino acid composition to be 0.733 $cm^3\ g^{-1}$ using the SEDNTERP software (John Philo), and the solvent density was 0.9985 g/cm^3. The degree of hydration of the totally unfolded protein was estimated based on the amino acid composition by the method of ref *19* according to ref *20*. The degree of hydration used for all calculations, 0.3793 g of H_2O/g of protein, was the result of correcting the calculated degree of hydration by a factor 0.7 (*21*).

The exact molecular weight of Ure2p C-terminal domain was determined by matrix-assisted laser desorption time-of-flight mass-analysis (MALDI-TOF, Bruker, Bremen, Germany) using α-cyano-4-hydroxycinnamic acid as matrix. Peptide sequence data for the Ure2p C-terminal domain were obtained by automated Edman degradation using a sequencer (model 470A or 477A; Applied Biosystems, Inc., Foster City, CA) equipped with an on-line phenylthiohydantoin amino acid analysis system (model 120A; Applied Biosystems, Inc.).

Electron Microscopy. Samples of full-length Ure2p as well as Ure2p C-terminal domain in their soluble or assembled forms were negatively stained on carbon-coated grids (200 mesh) with 1% uranyl acetate and examined in a Philips EM 410 electron microscope.

Proteolytic Digestions. Soluble full-length Ure2p as well as the Ure2p C-terminal domain (0.8 mg/mL) in 50 mM Tris, pH 7.5, 1 mM EGTA were treated at 37 °C by Proteinase K (2.4 μg/mL). Aliquots were removed at different time intervals following addition of the protease and transferred into Eppendorf tubes maintained at 90 °C containing sample buffer (50 mM Tris-HCl, pH 6.8, 4% SDS, 2% β-mercaptoethanol, 12% glycerol, 0.01% Serva Blue G, and 0.01% bromophenol blue) to arrest immediately the cleavage reaction. After incubation of each tube for 10 min at 90 °C, the samples were processed to monitor the time course of Ure2p cleavage by Tricine-SDS−polyacrylamide gel electrophoresis (*22*).

Fluorescence, Circular Dichroism, and Stopped Flow Measurements. The intrinsic fluorescence of Ure2p was recorded at 20 °C in a AMINCO-Bowman series 2 spectrofluorometer in 10 × 4 mm quartz cuvettes (Hellma) containing 400 μL of Ure2p solution. The excitation monochromator was set at 280 nm and the emission was recorded between 300 and 400 nm. The conformational changes of wild-type Ure2p, Ure2pW37 variant, and Ure2p C-terminal fragment were monitored by the decrease of tryptophan fluorescence (excitation 280 nm, emission 325 nm). Measurements were performed at 20 °C in a thermostated cuvette after overnight incubation of the proteins in the absence or the presence of GdmCl at 20 °C.

CD spectra were obtained with a J715 (Jasco) spectropolarimeter using a 0.1-cm path-length cuvette. All spectra were measured at 20 °C in 50 mM potassium phosphate buffer, pH 7.5, with or without guanidine hydrochloride.

Ure2p unfolding/dissociation was monitored using an excitation wavelength of 280 nm and an emission filter at 322 nm in a stopped-flow apparatus (DX.17 MV, Applied Photophysics) at 20 °C. The optical path was 1 cm, and the slits of the monochromator were 1 mm (4 nm bandwidth). One of the drive syringes contained the protein (0.5−5 μM) and the other drive syringe contained GdmCl (0−8 M).

Additional Methods. Protein concentrations were determined by either the Lowry (*23*) or the Bradford (*24*) methods. Alternatively, full-length Ure2p as well as Ure2p C-terminal domain concentrations were determined spectrophotometrically (HP 8453 diode array spectrophotometer, Hewlett-Packard). Congo Red binding was performed as described (*25*) and its birefringence checked as described (*11*). Standard SDS−polyacrylamide gel electrophoresis were performed in 10% gels following the method described by Laemmli (*26*).

RESULTS

Recombinant Ure2p C-Terminal Fragment is a Soluble Dimeric Protein. The strategy that was revealed successful for overexpressing full-length authentic Ure2p in *E. coli* (*9*) was applied to produce large amounts of Ure2p C-terminal fragment (Ure2p 94−354). Recombinant Ure2p 94−354 was purified to homogeneity through two chromatographic dimensions as described in Experimental Procedures. The molecular mass of the purified protein was determined using both SDS−PAGE and mass spectrometry. Recombinant Ure2p C-terminal fragment has an apparent molecular mass of 30 kDa by SDS−PAGE (not shown) close to its calculated molecular mass (29 932 Da). However, the actual molecular mass determined by mass spectrometry of 29 798 Da does not agree with the calculated molecular mass of Ure2p 94-354 but does match that of a polypeptide devoid of its N-terminal methionine residue (29 801 Da). Thus, the recombinant polypeptide appears to be subject to a cotranslational modification that results in the cleavage of the N-terminal methionine residue. Amino acid sequencing of Ure2p C-terminal fragment by automated Edman degradation gave the following sequence: SHVEYSRITK. This confirms the removal of the initiator methionine of Ure2p C-terminal domain probably cotranslationally by a prokaryotic methionine aminopeptidase (*27*).

Ure2p C-terminal fragment dimerizes in solution in agreement with ref *13*. Its apparent molecular mass, determined using size exclusion chromatography, is 80 kDa (not shown). Its sedimentation coefficient is $S_{20,W} = 3.97$, and its weight-average molecular weight measured by equilibrium sedimentation is 64 000 (not shown).

Ure2p C-Terminal Fragment is Highly Structured. Using various protease treatments, we previously showed that soluble full-length Ure2p is at least a two-domain protein (*9*). The major degradation product generated by proteinase K treatment of soluble full-length Ure2p was shown to have a molecular mass of about 30 kDa. This product is then degraded into shorter polypeptides (*9*). To assign these polypeptides to a part of Ure2p, full-length Ure2p and Ure2p 95−354 were subjected to proteinase K treatment and the reaction products were analyzed by SDS−PAGE. The data are presented in Figure 1. Soluble full-length Ure2p is rapidly cleaved into a product that has an apparent molecular mass of 29 kDa. Seven other peptides that have apparent molecular

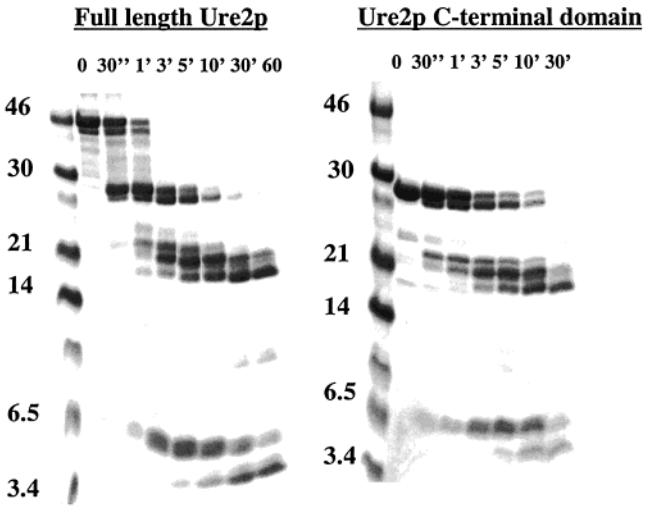

FIGURE 1: Full-length Ure2p degradation pattern is due to its C-terminal domain. The time courses of degradation of authentic Ure2p and Ure2p 95−354 by proteinase K were monitored by SDS electrophoresis followed by Coomassie staining. Time points are shown at the top of each gel. Molecular mass markers (in kDa) are shown on the left.

masses of 28, 24, 22, 21, 18, 6, and 4 kDa are generated upon further incubation. Identical peptides are generated upon cleavage of recombinant Ure2p 95−354, which has an apparent molecular mass of 29 kDa, by proteinase K. We conclude from this observation that the peptides generated upon proteinase K treatment of full-length Ure2p are exclusively derived from the C-terminal fragment of the protein. The low number of polypeptides that are generated upon protease treatment together with the fact that they appear to resist for prolonged periods of time strongly suggests that Ure2p 95−354 is structured into distinct domains. Furthermore, given that no additional peptides were found for full-length Ure2p as compared to Ure2p 95−354, we conclude that the N-terminal domain must rapidly degrade into peptides that are too short for detection by SDS−PAGE.

Ure2p 95−354 Self-Associates into High Molecular Weight Oligomers in Vitro. The capacity of Ure2p 95−354 to oligomerize into high molecular weight oligomers was assayed by three means. The first consisted of inducing self-association by bringing the pH of the solution containing Ure2p 95−354 to the isoelectric point of the protein (6.4); the second, by incubating Ure2p 95−354 for prolonged periods of time at 4 or 28 °C; and the third, by monitoring Congo Red binding and the subsequent green birefringence of polarized light that accompanies Congo Red binding. Ure2p 95−354 aggregation was followed spectrophotometrically and the oligomers analyzed by electron microscopy. Aggregation of Ure2p C-terminal fragment was instantaneous upon adjustment of the pH to 6.4 (Figure 2, panel A). In contrast, the kinetics of Ure2p 95−354 assembly at pH 7.5 at 4 or 28 °C (Figure 2, panel B) were slower, exhibiting a lag phase and an elongation phase preceding the onset of a

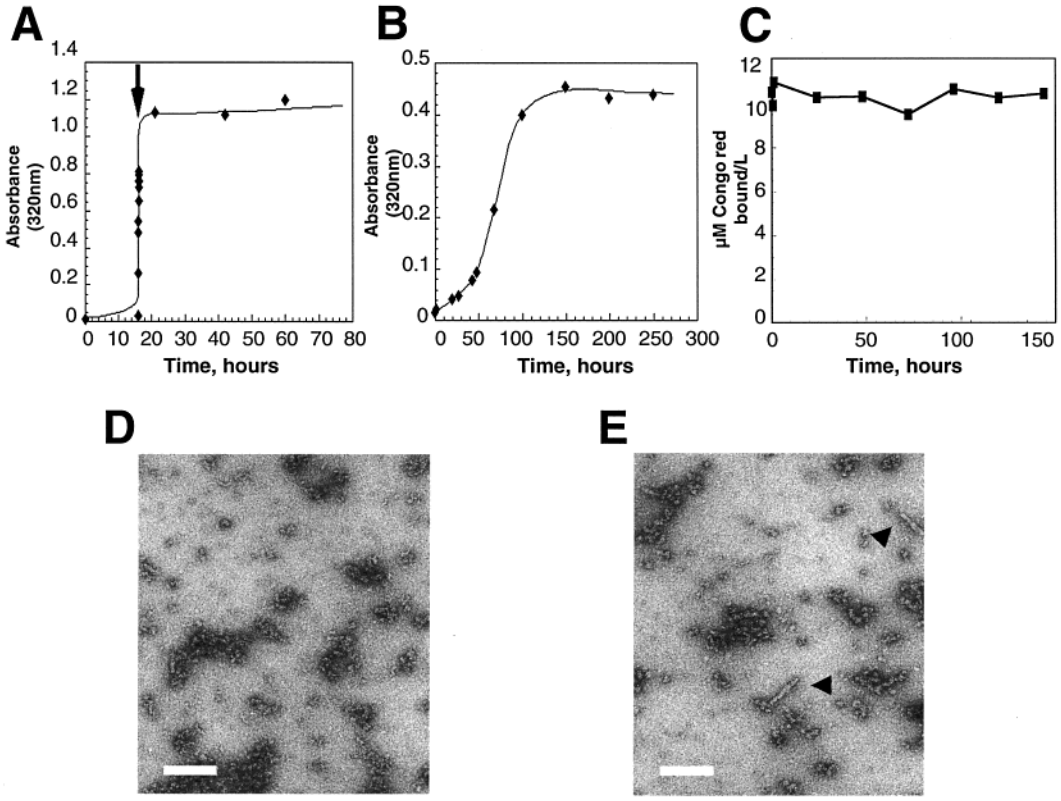

FIGURE 2: Assembly of Ure2p 95−354 into high molecular weight oligomers. (A) Kinetic of Ure2p 95−354 assembly monitored by measurement of the turbidity of the solution. The aggregation of Ure2p 95−354 in 20 mM Tris, pH 7.5, 100 mM KCl at 20 °C was induced at the time indicated by the arrow by adjustment of the pH of the solution to pH 6.5 by addition of HCl. (B) Time course of Ure2p 95−354 autoassembly followed by measurement of the turbidity of the solution at 20 °C in 20 mM Tris, pH 7.5, 100 mM KCl. (C) Binding of Congo Red to Ure2p 95−354 (85 μM) in 20 mM Tris, pH 7.5, 100 mM KCl. (D) Electron micrographs of negatively stained insoluble Ure2p 95−354 oligomers. No obvious elements of symmetry can be distinguished whithin these aggregates. (E) Electron micrographs of negatively stained oligomers obtained upon assembly of Ure2p 95−354 (7 μM) in the presence of authentic Ure2p (50 μM). The arrowheads indicate short amyloid fibrils. Bar = 200 nm in panel D and E.

plateau. Finally, Ure2p 95−354 aggregates were found to bind Congo Red in a noncooperative fashion (Figure 2, panel C). Binding of Congo Red is visible upon observation of sedimented aggregates using a light microscope. However, no green birefringence was observed under polarized light. This indicates that aggregated protein does not form amyloid structures.

Observation of negatively stained samples of Ure2p 95−354 aggregates obtained upon incubation of the protein at pH 6.4 or for prolonged periods of time revealed the presence of macromolecular structures, where no obvious element of symmetry can be distinguished (Figure 2, panel D).

To determine whether Ure2p C-terminal fragment has the capacity to incorporate into preformed amyloid fibrils, soluble Ure2p 95−354 (3 mg/mL) was incubated for various times (0−200 h) with increasing concentrations of soluble full-length Ure2p or preformed Ure2p fibrils (3−300 ng/mL), and the aggregates formed were examined in the electron microscope. At the highest full-length/Ure2p 95−354 ratio, very few fibrils were observed (Figure 2, panel E). However, the amorphous aggregates that were obtained under all conditions were identical to that formed in the absence of soluble full-length Ure2p or preformed Ure2p fibrils (Figure 2, panel D). Our data indicate that the formation of the unstructured aggregates appears not only to be uninfluenced by the addition of preformed Ure2p fibrils but concomitant to that of fibrils made of full-length Ure2p. We conclude from these data that Ure2p 95-354 is unable to interact with neither the soluble form nor the assembled form of full-length Ure2p. This underlines the central role of the N-terminal region of the protein in amyloid fibrils genesis.

Spectroscopic Properties and GdmCl-Dependent Refolding Transitions of Full-Length Ure2p and Ure2p 95−354. The overall secondary structure of full-length Ure2p and that of its C-terminal fragment were probed by circular dichroism (CD) spectroscopy. Ure2p 95−354 showed an α-helical content identical to that of full-length Ure2p (Figure 3, panel A). We conclude from these data that the tertiary structure of the protein is hardly affected by removal of Ure2p N-terminal fragment. The CD difference spectrum of full-length Ure2p and Ure2p 95−354 shown in Figure 3, panel B indicates that removal of the N-terminal fragment of the protein results in a large decrease of the ellipticity signal between 205 and 195 nm, consistent with the loss of a poorly structured domain.

Ure2p polypeptide chain has six tryptophan residues that are distributed throughout the C-terminal region of the protein. To monitor conformational changes occurring in the N-terminal region of the protein, a probe was designed in which the phenylalanine residue at position 37 was replaced by a tryptophan residue. The oligomeric state of Ure2pW37 variant was examined by analytical ultracentrifugation (Figure 4, panel A) and size-exclusion chromatography (Figure 4, panel B) and its capacity to form amyloid fibrils assayed by electron microscopy (Figure 4, panel C), measurement of Congo red binding (Figure 4, panel D) and Congo Red green birefringence under polarized light (not shown). The behavior of Ure2pW37 variant was found to be indistinguishable from that of wild-type Ure2p.

To test whether Ure2p N-terminal region influences the stability of the protein, the equilibrium unfolding transitions

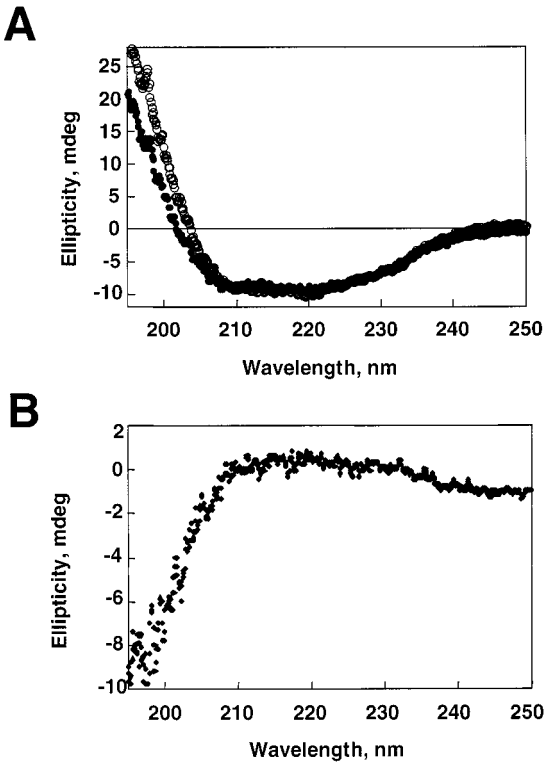

FIGURE 3: Ure2p N-terminal region is poorly structured. (A) Far UV CD spectra of 0.25 μM authentic Ure2p (●) and 0.25 μM Ure2p 95−354 (○) in 50 mM KPO_4 buffer, pH 7.5. (B) CD difference spectrum between the two forms of the protein is presented in panel A.

of full-length Ure2p and Ure2p 95−354 by GdmCl were measured using the intrinsic fluorescence of the protein as a probe at various pH. At pH 8.4, full-length Ure2p as well as Ure2p 95−354 show a one-step unfolding transition with a midpoint for unfolding of 2.7 M GdmCl (Figure 5, panel A). These observations are in agreement with the results of Perret et al. (*13*). Evidences for equilibrium unfolding intermediates were found when equilibrium unfolding transition measurements were performed under experimental conditions that were not explored by Perret et al. (*13*), i.e., pH 7.5 and 5.5. Under these conditions, full-length Ure2p as well as Ure2p 95−354 unfolding show two transitions. At pH 7.5, the midpoint of the first transition is 1.6 M GdmCl, while that of the second transition is 2.7 M GdmCl (Figure 5, panel B). Authentic Ure2p and Ure2p 95−354 appear much less stable at pH 5.5 given that the midpoint of the first transition is 0.75 M GdmCl while that of the second transition stays identical to that observed at pH 8.5 and 7.5, i.e., 2.7 M GdmCl (Figure 5, panel C). Interestingly, the first unfolding transition at pH 7.5 is protein concentration independent over a 50-fold protein concentration range (0.3 to 15 μM) indicating a change in the tertiary structure of the polypeptide that yields a partially unfolded dimeric intermediate (i.e., $N_2 \rightarrow I_2$). The second unfolding transition is concentration-dependent, which strongly suggests a dissociation of the dimeric folding intermediate into a monomeric form (M) of the protein (i.e., $I_2 \rightarrow 2 \times M$).

The kinetics of Ure2p denaturation were measured using a stopped-flow apparatus. The best fit to the data was found by using the equation: $A1 \cdot 10^{-k1x} + A2 \cdot 10^{-k2x} + A0$ with the following values for the pseudo first-order rate constants $k1 = 0.762\ s^{-1}$ and $k2 = 0.131\ s^{-1}$ (Figure 5, panel D).

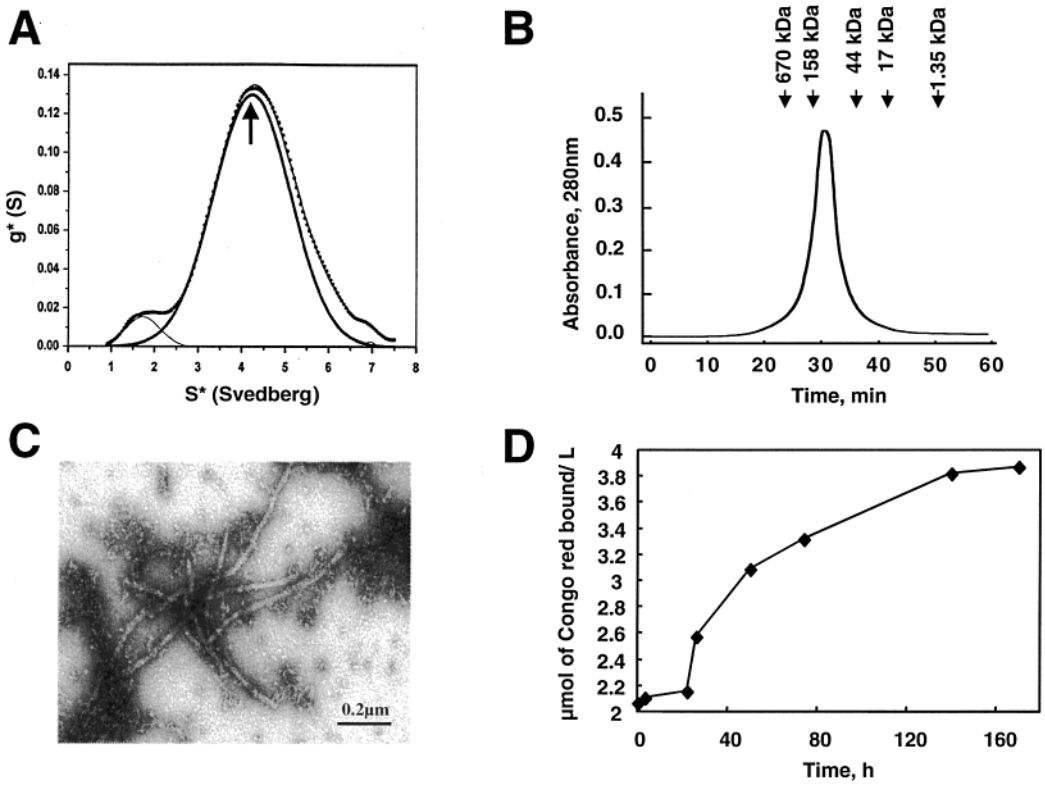

FIGURE 4: Quaternary structure of Ure2p W37 variant. (A) Distribution of sedimentation velocity of Ure2p W37 variant (0.5 mg/mL). The arrow indicates the position of the maximum of g*(s), 4.2*S*. The solid lines represents the best fit obtained to the data points (●) using a monomer−dimer model. Rotor speed 60 000 rpm, temperature 20 °C. (B) Elution profile of pure recombinant Ure2p W37 variant from a superose 6 (HR 10/30) column. Arrows show the location of molecular size markers (thyroglobulin, 670 kDa; immunoglobulin G, 158 kDa; ovalbumin, 44 kDa; myoglobin, 17 kDa; and vitamin B12, 1.35 kDa) run under identical conditions on the same column. (C) Electron micrographs of negatively stained oligomers made of Ure2p W37 variant are shown. The soluble form of Ure2p W37 variant (30 μM) in 20 mM Tris, pH 7.5, 100 mM KCl autoassembles into fibrils. Bar = 0.2 μm. (D) Time course of assembly of Ure2p W37 variant (20 μM) in 20 mM Tris, pH 7.5, 100 mM KCl into amyloid fibrils monitored by measurement of the binding of Congo Red.

In contrast with the findings of Perret et al. (*13*), denaturation of authentic Ure2p and Ure2p 95−354 was irreversible as judged by the regain of fluorescence and light scattering measurements. Indeed, under all the conditions explored in this study, within a protein concentration range of 0.2 to 15 μM, equilibrium renaturation experiments revealed the oligomerization of unfolded Ure2p and Ure2p 95−354 into large aggregates that scatter light (not shown).

Finally, the species present at various GdmCl concentrations were characterized by analytical ultracentrifugation and CD measurements. The sedimentation velocity data are summarized in Table 1 and indicate that the species present in the absence of GdmCl is a dimeric form of the protein, while the species present at high GdmCl concentration (4.5 M) is a monomeric form of the protein. At a concentration of GdmCl equal to that where the second unfolding transition occurs (2.7 M), Ure2p aggregates into a species that has a sedimentation coefficient of 20*S*. The far UV CD spectra of full-length Ure2p and Ure2p 95−354 in the absence or the presence of 2 and 5 M GdmCl are presented in Figure 6, panels A and B. These are the conditions where Ure2p is partially and fully unfolded. Both proteins unfold partially in the presence of 2 M GdmCl as attested by the decrease in the CD signal. At higher GdmCl concentrations (5 M), the polypeptide chains unfold completely and dissociate as demonstrated by the total loss of their α-helical content. To further determine whether the unfolding intermediate in Figures 5 and 6 is still folded, its proteolysis pattern upon treatment with proteinase K was compared to that of native Ure2p. Native and partially unfolded Ure2p degrade at similar rates. In addition, similar degradation products are generated (Figure 6, panels C and D). This indicates that Ure2p unfolding intermediate is partially folded. However, a 29-kDa polypeptide, generated upon treatment of native Ure2p by proteinase K, corresponding to Ure2p C-terminal region, is rapidly degraded upon partial unfolding of the protein by GdmCl. This is consistent with an increased exposure of cleavage sites in Ure2p C-terminal region.

We conclude from our observations that Ure2p unfolding is a two-step process. The fact that the same unfolding intermediate is observed for full-length Ure2p and Ure2p 95−354 suggests that the folding intermediate generated upon partial unfolding of full-length Ure2p is similar to that generated upon treatment of Ure2p 95−354 by the same concentration of GdmCl. Thus, this observation can be attributed to the C-terminal domain of the protein. Our observations are consistent with the first step being a partial unfolding of the protein, and the second transition being the dissociation of the dimeric form of Ure2p into a monomeric form as demonstrated by the analytical ultracentrifugation measurements. We further conclude that Ure2p N-terminal region does not stabilize Ure2p during the unfolding process.

The influence of the N-terminal region of Ure2p on the stability of the protein was further examined by GdmCl-dependent equilibrium unfolding measurements using the Ure2pW37 variant as a probe. Ure2pW37 equilibrium

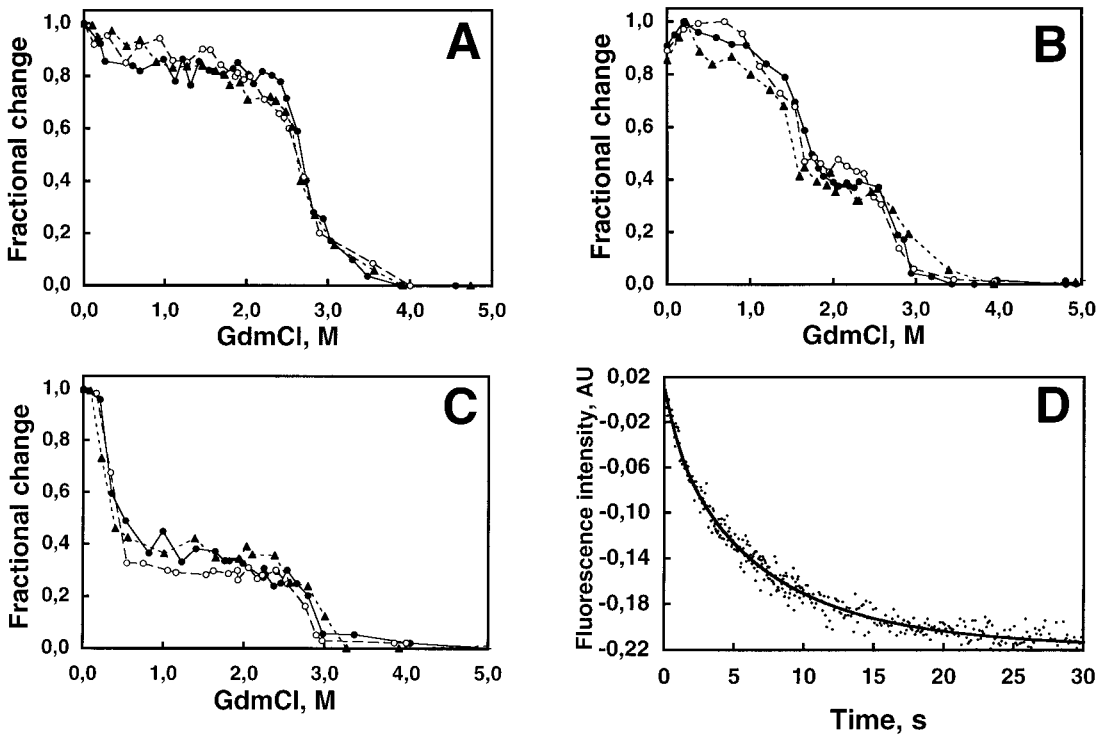

FIGURE 5: Equilibrium denaturation curves of authentic Ure2p, Ure2p W37 variant, and Ure2p 94−354. GdmCl-induced unfolding transitions of full-length Ure2p (0.5 μM, ●), Ure2p W37 variant (0.5 μM, ▲), and Ure2p 95−354 (0.5 μM, ○) at pH (A) 8.4, (B) 7.5, and (C) 5.5 and 20 °C were monitored by measurement of the intrinsic fluorescence of the proteins. GdmCl concentrations were determined by refractometry. (D) Kinetic analysis of full-length Ure2p denaturation (2.5 μM in 20 mM Tris, pH 7.5, 100 mM KCl) in the presence of 4 M GdmCl monitored in the stopped-flow apparatus as described in the material and methods section. Values of rate contants were adjusted to obtain the best fit of simulated kinetic curves to the experimental data (●).

Table 1: Oligomeric State of Full-Length Ure2p during Equilibrium Denaturation at Various pHs[a]

	species ($s^{\circ}_{20,w}$) at various pH		
GdmCl (M)	5.5	7.5	8.5
0	30−60 (99%)	4.5 (98%)	5.0 (99%)
2.5	nd	21 (87%)	20 (60%)
		5.0 (13%)	2.6 (40%)
4.5	nd	2.6 (92%)	2.6 (86%)
		5.0 (8%)	5.0 (14%)

[a] Sedimentation velocity experiments were performed at 20 °C at 45000 and 60000 rpm. Full-length Ure2p (10 μM) was incubated overnight at 20 °C in the absence or the presence of GdmCl in the following buffers: 50 mM potassium acetate, pH 5.5, 50 mM KCl, 1 mM EGTA; 50 mM potassium phosphate, pH 7.5, 50 mM KCl, 1 mM EGTA; 50 mM Tris, pH 8.5, 50 mM KCl, 1 mM EGTA; nd: nondetermined.

unfolding transitions at pH 8.5 (Figure 5, panel A), 7.5 (Figure 5, panel B), and 5.5 (Figure 5, panel C) are superimposable to that of authentic Ure2p and Ure2p 95-354 showing the same transitions with midpoints at 1.6 M and 2.7 M GdmCl at pH 7.5.

Assembly of Ure2p into Amyloid Fibrils. Amyloid formation is widely believed to be a generic property of polypeptide chains. It is also believed that the form of a given protein that assembles into amyloid fibrils is a partially unfolded polypeptide chain. The fact that only a subset of proteins has the capacity to form such polymers has been attributed to an insufficient amount of folding intermediate that plays the role of amyloid precursor (*28*). We previously showed that authentic Ure2p assembles into amyloid fibrils (*9*). To further document the mechanism of Ure2p assembly into amyloid fibrils, we examined the capacity of the folding intermediate of Ure2p identified above and that of monomeric Ure2p to assemble into amyloid fibrils. The assembly kinetics for the native, partially unfolded and fully unfolded forms of the protein were analyzed by electron microscopy, Congo Red binding, and green birefringence under polarized light associated to Congo Red binding. The first amyloid fibrils appeared upon incubation of the native form of Ure2p for 3 h at 4 °C. These fibrils increased in number and length with time. No similar fibrils were visible 100 h after the onset of the incubation of Ure2p unfolding intermediate or fully unfolded form generated in the presence of 2.2 and 4 M GdmCl, respectively. Instead, short oligomers (30 × 8 nm) were observed in the presence of 2.2 M GdmCl. This indicates that the unfolding intermediate that forms in the presence of 2.2 M GdmCl is not a potential precursor to amyloid fibrils.

The capacity of authentic Ure2p to assemble into amyloid fibrils at various pH was also examined. Amyloid fibrils were generated at pH 7.5 (Figure 7, panel A), 6.5 (Figure 7, panel B), and 5.5 (Figure 7, panel C), whereas large aggregates where no obvious element of symmetry can be distinguished were obtained at pH 8.5 (Figure 7, panel D). This indicates that pH-induced conformational changes direct Ure2p assembly into amyloid fibrils or amorphous aggregates. Strikingly, Ure2p amorphous aggregates obtained at pH 8.5 disassemble in the presence of 2.5 M GdmCl while Ure2p fibrils obtained at pH 7.5 or 5.5 persist in the presence of 4 M GdmCl and were found to disassemble at concentrations of GdmCl above 5 M. This strongly suggests that the interacting surfaces between Ure2p molecules that drive

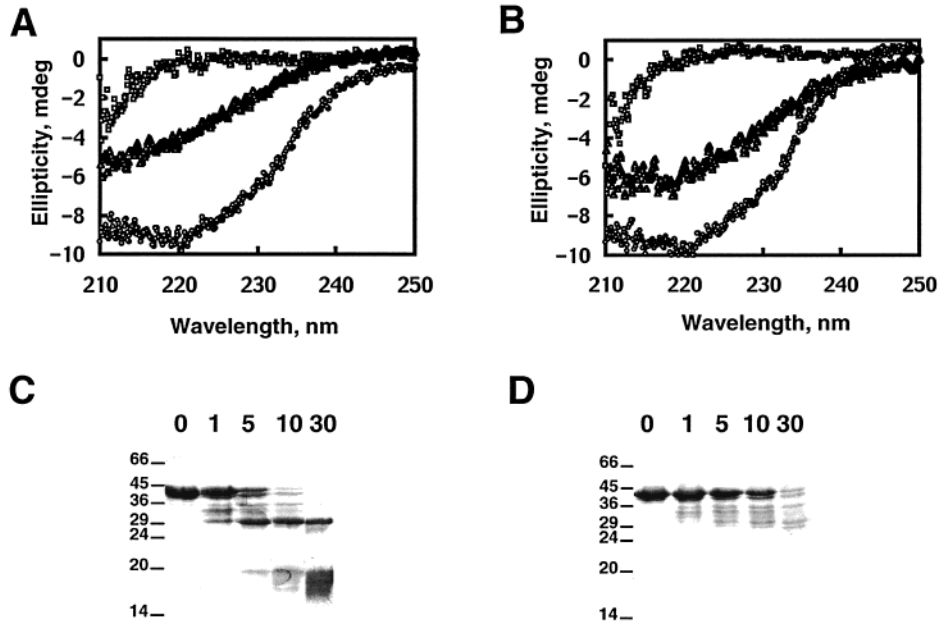

FIGURE 6: Unfolding of Ure2p by guanidinium chloride yields unfolding intermediates that possess tertiary structure elements. Far UV circular dichroism spectra of authentic Ure2p (0.25 μM) (A) and Ure2p 95−354 (0.25 μM) (B) in 50 mM KPO_4 buffer, pH 7.5 at 20 °C, in the absence (○) or the presence of 2 (△) and 5 M (□) GdmCl. Proteinase K degradation profiles of native (C) and GdmCl partially unfolded (D) full-length Ure2p (25 μM).

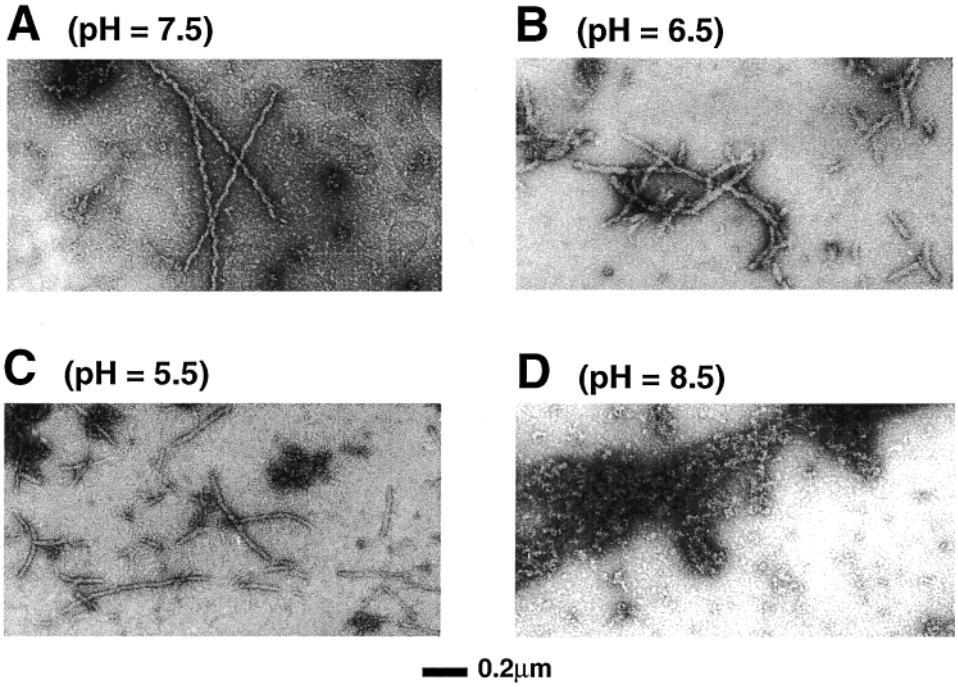

FIGURE 7: Characterization of Ure2p oligomers that form at various pHs. Electron micrographs of negatively stained Ure2p oligomers obtained under various pH conditions (A) 20 mM Tris, pH 7.5, 100 mM KCl; (B) 20 mM MES, pH 6.5, 100 mM KCl; (C) 20 mM potassium acetate, pH 5.5, 100 mM KCl; (D) 20 mM Tris, pH 8.5, 100 mM KCl. Bar = 0.2 μm.

the assembly into either amorphous aggregates or amyloid fibrils are different.

We conclude from these results that Ure2p assembly into amyloid fibrils is unfavored upon partial unfolding or dissociation of the dimeric form of the protein. The fact that the equilibrium unfolding patterns of full-length Ure2p, Ure2pW37 variant, and Ure2p 95−354 by GdmCl are identical suggests that the unfolding intermediate or monomeric forms of the protein generated under these experimental conditions are identical and characteristic of the unfolding/dissociation of Ure2p C-terminal domain. The latter conclusion is consistent with the finding that Ure2p 95−354 does not assemble into amyloid fibrils also with the fact that the N-terminal domain of the protein is essential for amyloidogenesis in vitro (*11*, *12*).

DISCUSSION

Yeast prions are very useful tools to document not only the molecular mechanisms at the origin of the advent and propagation of prion neurodegenerative diseases such as

transmissible spongiform encephalopathies but also that of nonprion neurodegenerative diseases such as Huntington's disease.

The yeast prion Ure2p is a two-domain protein (*8*, *9*, *13*). The poorly structured N-terminal region of the protein which has an unusual amino acid composition (43 amino acid residues out of 94 are asparagine and glutamine residues) is structurally homologous to Huntingtin (*29*) and required for the assembly of the protein into amyloid fibrils. The C-terminal region of the protein is involved in nitrogen regulation in yeast. A number of observations have led to the view that the N- and C-terminal regions of Ure2p interact specifically when covalently attached (*7*, *8*, *15*, *30*). It has also been proposed that this interaction confers a higher degree of stability to the N-terminal region of Ure2p (*7*, *8*, *30*). The latter hypothesis strongly suggests that the interaction of the two regions of the protein regulate the overall capacity of Ure2p to switch from the native soluble form to the amyloid insoluble form.

Perret and co-workers (*13*) have reported that the unfolding of His-tagged Ure2p is fully reversible. In addition, the single unfolding transition observed by these authors is concentration dependent. Here we demonstrate that the Ure2p N-terminal region has no effect on the overall stability of the protein. We also show that Ure2p unfolding is irreversible and bring evidence for a stable unfolding intermediate.

Properties of Ure2p Domains. To determine the stability, conformation, and assembly properties of Ure2p domains, the N- and C-terminal fragments of the protein were expressed separately.

Ure2p N-terminal region degrades whether it is expressed alone or fused to an intein-chitin binding domain chimera for rapid purification purpose. Ure2p C-terminal fragment was overproduced and purified. Ure2p 95−354 dimerizes in solution as does authentic Ure2p. The polypeptide chain is compact and structured into domains. Its degradation pattern by proteinase K is identical to that of full-length Ure2p which demonstrates that the proteolytic pattern is due to polypeptides belonging to Ure2p C-terminal fragment. Using the crystal structure of Ure2p that we recently solved (*31*) we propose that proteinase K cleavage of Ure2p 95−354 is sequential. Cleavage occurs within exposed loops around amino acid residues 325, 285, 275, and 115.

Ure2p 95−354 assembles into insoluble high molecular weight oligomers where no obvious elements of symmetry are distinguishable. Thus, indicating that removal of Ure2p N-terminal region abolishes the capacity of the protein to assemble into preformed amyloid fibrils.

Structure of Ure2p. A number of studies have led to the view of a possible interaction between the flexible N-terminal region of Ure2p and the compactly folded C-terminal region of the protein (*7*, *8*, *15*, *30*). The question of whether Ure2p N-terminal fragment plays a role in the stability and the functional tertiary structure of the protein is crucial since its issue may allow a better understanding of the mechanisms of Ure2p assembly into amyloid fibrils. We have investigated this point using equilibrium unfolding measurements performed on authentic Ure2p, Ure2p 95−354, and Ure2p W37 variant at various pHs. Our data indicate that denaturation of Ure2p by GdmCl is irreversible in disagreement with the data of Perret et al. (*13*) obtained using His-tagged Ure2p. Equilibrium unfolding measurements performed under pH conditions where Ure2p assembles into amyloid fibrils show unequivocally two transitions while single transitions were observed under conditions where the protein does not assemble into amyloid fibrils, e.g., pH 8.4. The first transition is concentration independent. It is due to the partial unfolding of Ure2p dimers. The second transition is concentration dependent. It is the result of the dissociation of Ure2p dimer and the complete unfolding of the polypeptide chains. The single transition observed at pH 8.4 indicates that unfolding and dissociation of Ure2p dimer are concomitant while the two reactions are uncoupled in the pH range where amyloid fibrils are generated. These conclusions are supported by the X-ray structure of Ure2p (*31*). While W202 and W316 are involved into interactions between the two domains of Ure2p 95−354, W179 and W215 are located in the dimeric form of Ure2p at the interface between two monomers.

Amyloidogenesis. It has been reported that Ure2p forms large aggregates when yeast cells exhibit [URE3] phenotype (*10*). It is not clear whether these aggregates are amyloid fibrils packed in bundles. Nonetheless, the ability of Ure2p to assemble in vitro into amyloid fibrils argues strongly in favor of the existence of such polymers in vivo.

Ure2p N-terminal region appears to play a central role in amyloidogenesis. It has not yet been possible to document its conformational changes because of its high sensitivity to degradation. Our data indicate that the conformational state that plays the role of "precursor" for amyloid fibrils involves Ure2p N-terminal region in a state that exists under neutral or acidic pH conditions. In light of the crystal structure of Ure2p (*31*), the N-terminal region of one Ure2p monomer appears to be in the vicinity of a flexible α-helice belonging to the partner polypeptide chain in Ure2p dimer. This could have consequences on the sharp regulation of the conformational state of Ure2p N-terminal region. Consequently, efforts to express and purify Ure2p N-terminal domain labeled in a way that may allow us to document its conformational changes have to be designed to assess the molecular mechanism of Ure2p assembly into amyloid fibrils.

ACKNOWLEDGMENT

We thank Pr. Joël Janin for his support and Prs. Rainer Jaenicke, Ineke Braakman, Robley Williams, and Solange Morera for helpful discussions. We are grateful to Dr. Virginie Redeker for her help in microsequencing and mass spectrometry measurements and to Mr. Gérard Batelier for his help in analytical ultracentrifugation experiments.

REFERENCES

1. Lindquist, S. (1997) *Cell 89*, 495−498.
2. Lacroute, F. (1971) *J. Bacteriol. 106*, 519−522.
3. Aigle, M., and Lacroute, F. (1975) *Mol. Gen. Genet. 136*, 327−335.
4. Wickner, R. B., Edskes, H. K., Maddelein, M. L., Taylor, K. L., and Moriyama, H. (1999) *J. Biol. Chem. 274*, 555−558.
5. Wickner, R. B. (1994) *Science 264*, 566−569.
6. Prusiner, S. B. (1997) *Science 278*, 245−251.
7. Masison, D. C., and Wickner, R. B. (1995) *Science 270*, 93−95.
8. Masison, D. C., Maddelein, M. L., and Wickner, R. B. (1997) *Proc. Natl. Acad. Sci. U.S.A. 94*, 12503−12508.

9. Thual, C., Komar, A. A., Bousset, L., Fernandez-Bellot, E., Cullin, C., and Melki, R. (1999) *J. Biol. Chem. 274*, 13666−13674.
10. Edskes, H. K., Gray, V. T., and Wickner, R. B. (1999) *Proc. Natl. Acad. Sci. U.S.A.* 96, 1498−1503.
11. Taylor, K. L., Cheng, N., Williams, R. W., Steven, A. C., and Wickner, R. D. (1999) *Science 283*, 1339−1343.
12. Schlumpberger, M., Wille, H., Balwin, M. A., Butler, D. A., Herskowitz, I., and Prusiner, S. B. (2000) *Protein Sci. 9*, 440−451.
13. Perret, S., Freeman, S. J., Butler, J. G., and Fersht, A. R. (1999) *J. Mol. Biol. 290*, 331−345.
14. Coschigano, P. W., and Magasanik, B. (1991) *Mol. Cell. Biol. 11*, 822−832.
15. Fernandez-Bellot, E., Guillemet, E., Baudin-Baillieu, A., Gaumer, S., Komar A. A., and Cullin, C. (1999) *Biochem. J. 338*, 403−407.
16. Komar, A. A., Lesnik, T., Cullin, C., Guillemet, E., Ehrlich, R., and Reiss, C. (1997) *FEBS Lett. 415*, 6−10.
17. Philo, J. S. (1994) Measuring sedimentation, diffusion, and molecular weights of small molecules by direct fitting of sedimentation velocity concentration profiles. In *Modern Analytical Ultracentrifugation* (Schuster, T. M., and Laue, T. M., Eds.) pp 156−170, Birkhäuser, Boston.
18. Stafford, W. F., III. (1992) *Anal. Biochem. 203*, 295−301.
19. Kuntz, I. D. (1971) *J. Am. Chem. Soc. 93*, 516−518.
20. Laue, T. M., Shah, B. D., Ridgeway, T. M., and Pelletier, S. L. (1992) Computer-aided interpretation of analytical sedimentation data for proteins. In *Analytical ultracentrifugation in Biochemistry and Polymer Sciences* (Harding, S. E., Rowe, A. J., Horton, J. C., Eds.) pp 90−125, The Royal Society of Chemistry, Cambridge, United Kingdom.
21. Lin, T. H., Quinn, T., Walsh, M., Gradgennet, D., and Lee, J. C. (1991) *J. Biol. Chem. 266*, 1635−1640.
22. Schaegger, H., and von Jagow, G. (1987) *Anal. Biochem. 166*, 368−379.
23. Lowry, O. H., Rosebrough, N. J., Farr, A. L., and Randall, R. J. (1951) *J. Biol. Chem. 193*, 265−275.
24. Bradford, M. M. (1976) *Anal. Biochem. 72*, 248−254.
25. Glover, J. R., Kowal, A. S., Schirmer, E. C., Patino, M. M., Liu, J. J., and Lindquist, S. (1997) *Cell 89*, 811−819.
26. Laemmli, U. K. (1970) *Nature 227*, 680−685.
27. Ben-Bassat A., Bauer K., Chang S. Y., Myambo K., Boosman A., and Chang S. (1987) *J. Bacteriol. 169*, 751−757.
28. Dobson, C. M. (1999) *Trends Biochem. Sci. 24*, 329−332.
29. Perutz, M. F. (1999) *Trends Biochem. Sci. 24*, 58−63.
30. Maddelein, M. L., and Wickner, R. B. (1999) *Mol. Cel. Biol. 19*, 4516−4524.
31. Bousset, L., Belrhali, H., Janin, J., Melki, R., and Morera, S. (2001) *Structure 9*, 39−46.

BI001916L